Sausage oscillations of coronal plasma structures

V. M. Nakariakov

Physics Department, University of Warwick, Coventry, CV4 7AL, UK

Central Astronomical Observatory at Pulkovo of the Russian Academy of Sciences, 196140 St Petersburg, Russia

V.Nakariakov@warwick.ac.uk

and

C. Hornsey

Physics Department, University of Warwick, Coventry, CV4 7AL, UK

and

V. F. Melnikov

Central Astronomical Observatory at Pulkovo of the Russian Academy of Sciences, 196140 St Petersburg, Russia

ABSTRACT

Dependence of the period of sausage oscillations of coronal loops on its length and the radial profile depth and steepness is determined. We performed a parametric study of linear axisymmetric fast magnetoacoustic (sausage) oscillations of coronal loops modelled as a field-aligned low-β plasma cylinder with a smooth inhomogeneity of the plasma density in the radial direction. The density decreases smoothly in the radial direction. Sausage oscillations are impulsively excited by a perturbation of the radial velocity, localised at the cylinder axis and having a harmonic dependence on the longitudinal coordinate. The initial perturbation results either in a leaky or trapped sausage oscillation, depending upon whether the longitudinal wavenumber is smaller or greater than a cut-off value, respectively. The period of the sausage oscillations was found to always grow with the increase in the longitudinal wavelength, with the saturation of this dependence in the long-wavelength limit. Deeper and steeper radial profiles of the Alfvén speed correspond to more efficient trapping of sausage modes: the cutoff value of the wavelength increases with the steepness and the density (or Alfvén speed)

contrast ratio. In the leaky regime, the period is always longer than the period of a trapped mode of a shorter wavelength in the same cylinder. For shallow profiles of the density and shorter wavelengths, the period grows with the wavelength. In the long wavelength limit, the period becomes independent of the wavelength, and increases with the depth and steepness of the radial profile of the Alfvén speed.

Subject headings: Sun: oscillations — Sun: flares — Sun: X-rays, gamma rays — Sun: radio radiation

1. Introduction

The theoretical foundation of magnetohydrodynamic (MHD) coronal seismology, the rapidly developing branch of solar physics that uses MHD waves and oscillations for the diagnostics of the plasma, is the theory of MHD oscillations of a plasma cylinder (see, e.g. Banerjee et al. 2007; De Moortel & Nakariakov 2012; Stepanov et al. 2012, for recent reviews). This model describes adequately standing and propagating MHD waves in various plasma structures of the solar corona, such as loops and various filaments. In the low-β plasma, typical for coronal active regions, a plasma cylinder embedded in a plasma with different properties has four main modes: the torsional, kink, sausage and longitudinal (e.g. Zaitsev & Stepanov 1975, 1982; Edwin & Roberts 1983). These modes have very different physical properties and different observational manifestations. The sausage mode, also known as an $m = 0$ or peristaltic mode, is a sequence of expansions and contractions of the cross-section of the cylinder, accompanied by the variation of the plasma density and of the absolute value of the magnetic field. In a low-β case the plasma flows in the sausage mode are predominantly transverse, in the radial direction (e.g. Gruszecki et al. 2012).

Initially, the interest in the sausage mode was associated with the medium-period quasi-periodic pulsations observed in flaring energy releases (e.g. Rosenberg 1970; Zaitsev & Stepanov 1982; Nakariakov & Melnikov 2009). The first direct spatially-resolved observational detection of a sausage oscillation of a flaring loop was made in the gyrosynchrotron and soft X-ray emission (Nakariakov et al. 2003; Melnikov et al. 2005). Detailed analysis of the possible examples of sausage oscillations showed good spatial coherence of the oscillatory signals over the whole loop spatially resolved in the microwave band (Inglis et al. 2008). Such a spatial structure is consistent with sausage mode, while alternative interpretation, e.g. in terms of the "dripping" model (Nakariakov & Melnikov 2009) cannot be excluded. Analysis of the optical emission from a cool post-flare loop revealed the possible presence of the global (fundamental) sausage mode as well as its second spatial harmonics (Srivastava et al.

2008). Sausage oscillations could also be responsible for the intensity oscillations observed in the gradual phase of a white-light flare on the RS CVn binary II Peg (Mathioudakis et al. 2003). Very recently, periodic variations of the EUV emission were also interpreted in terms of sausage oscillations (Van Doorsselaere et al. 2011; Su et al. 2012). In the interpretation it is important to pay attention to the line-of-sight integration effect, as it was recently pointed out in (Mossessian & Fleishman 2012; Gruszecki et al. 2012). In particular, for a line-of-sight perpendicular to the oscillating cylinder and for a spatial resolution of the order of the diameter of the cylinder or poorer, the intensity perturbations produced by a sausage mode in the optically-thin emission regime are negligible.

Theoretical modelling of sausage modes of coronal structures has a long history. Sausage modes are highly dispersive, with their properties being dependent upon the longitudinal wavenumber (e.g. Zaitsev & Stepanov 1982; Edwin & Roberts 1983; Roberts et al. 1984; Selwa et al. 2004). Depending upon the ratio of the longitudinal wavelength (determined, e.g., in the case of standing waves by the length of the oscillating loop) to the radius of the plasma cylinder, the mode can be either trapped or leaky. Trapped modes experience the total internal reflection at the cylinder surface and are evanescent outside the loop. The period of the standing trapped sausage modes, i.e. in dense and thick flaring loops, grows with the wavelength (Nakariakov et al. 2003; Aschwanden et al. 2004). Sausage modes of longer wavelengths leak from the cylinder, forming a train of outwardly-propagating fast magnetoacoustic waves outside the cylinder. This mechanism of wave leakage is intrinsic and different from the tunnelling caused by non-uniformity of the external medium (see, e.g. Verwichte et al. 2006). The threshold value of the ratio of the longitudinal wavelength to the radius of the cylinder is defined by the ratio of the fast magnetoacoustic speeds inside and outside the cylinder (Zaitsev & Stepanov 1982; Edwin & Roberts 1983). Such a behaviour was found to be weakly sensitive to the smoothness of the transverse profile of the fast speed (Pascoe et al. 2007b), fine structuring in the form of multiple coaxial shells (Pascoe et al. 2007a), longitudinal variation of the cylinder cross-section (Pascoe et al. 2009), and finite-β effects (Inglis et al. 2009).

However, sausage modes are still not entirely understood. In particular, the dependence of the time period on the longitudinal wavelength in the leaky regime, which is information crucial for the development of seismological techniques based upon this mode, is still debated. On one hand, analysis of dispersion relations for linear sausage perturbations clearly showed that in the long-wavelength regime the period of leaky sausage modes is independent of the wavelength (e.g. Zaitsev & Stepanov 1982; Kopylova et al. 2002, 2007) and is determined by the ratio of the radius of the cylinder to the internal value of the fast speed. On the other hand, it was argued that the gradual increase in the wavelength from a trapped regime value should lead to the growth of the period (Nakariakov et al. 2003; Aschwanden et al. 2004) for a

fixed value of the radius of the cylinder. Moreover, numerical simulations of the initial value problem demonstrated that the period of the mode grows with the wavelength (e.g. Pascoe et al. 2007b; Inglis et al. 2009) in both trapped and leaky regimes. The situation is complicated by the difficulties with the search for the complex roots of transcendental algebraic equations, representing the dispersion relations, analytically (Ruderman & Roberts 2006).

In this paper we aim to resolve this long-standing discrepancy. We perform analysis of an initial value problem, considering the evolution of an axially-symmetric perturbation of a straight plasma cylinder embedded in a uniform magnetic field, similar to the works of (Pascoe et al. 2007b; Inglis et al. 2009; Gruszecki et al. 2012). In contrast with (Pascoe et al. 2007b; Inglis et al. 2009) where a plane plasma slab was considered, we study sausage modes of a plasma cylinder. Moreover, we extend the range of the problem parameters, considering the ratio of the length of the perturbed cylinder to its diameter up to 60 and the ratio of the Alfvén speeds outside and inside the cylinder up to 20. In the previous studies these parameters were considered up to 15 and 7, respectively (Inglis et al. 2009). In addition, we study the dependence of the sausage mode period on the steepness of the transverse profile of the plasma in the cylinder.

We consider a radially-nonuniform plasma cylinder embedded in a uniform and straight magnetic field in the zero-β regime. We perform a parametric study of the sausage mode of this plasma equilibrium, varying the contrast of the Alfvén (fast magnetoacoustic) speed inside and outside the cylinder, and the steepness of the plasma non-uniformity in the radial direction. We consider, for the first time, the transition from the short-wavelength trapped regime to the long-wavelength regime, investigating how the dependence of the period on the wavelength evolves to its independence.

2. Numerical model

Consider a smooth cylinder of a zero-β plasma, stretched along a uniform magnetic field B_0 directed in the z direction. The density of the plasma ρ_0 decreases with the radial coordinate r. This is a standard setup for modelling sausage oscillations of coronal loops, see, e.g., Fig. 1 and 2 of Pascoe et al. (2007a). The Alfvén speed (that coincides with the fast speed in this limit) increases in the radial direction and is modelled by the function

$$C_A(r) = B_0/\sqrt{\mu_0\rho_0(r)} = C_{A\infty}\left[1 - \delta\exp\left(-\frac{r^\alpha}{d^\alpha}\right)\right], \tag{1}$$

where $C_{A\infty}$ is the Alfvén speed at infinity, $0 < \delta < 1$ is the decrease in the speed at the axis of the cylinder, $\alpha > 1$ is the index of the steepness of the profile and d is an effective

radius of the cylinder (see Fig. 1), and μ_0 is the vacuum permeability. The Alfvén speed then is $C_{A0} = C_{A\infty}(1-\delta)$ at the cylinder axis. Thus, varying the parameters of δ and α we change the contrast ratio $C_{A0}/C_{A\infty}$ and the steepness of the radial profile, respectively. As the magnetic field is uniform and the gas pressure is taken to be negligible, the equilibrium total pressure is constant everywhere. Hence, the parameter $\delta = 1 - C_{A0}/C_{A\infty}$ is connected with the contrast of the equilibrium plasma density ρ_0 in the cylinder centre and at infinity, as $\delta = 1 - [\rho_0(\infty)/\rho_0(0)]^{1/2}$. The case of the infinitely steep profile, $\alpha \to \infty$, corresponds to the Edwin & Roberts (1983) model with the step-function profile.

In this study we restrict our attention to dissipation-less processes, described by ideal MHD,

$$\rho \frac{d\,\mathbf{V}}{d\,t} = -\frac{1}{\mu_0}\mathbf{B} \times \mathrm{curl}\mathbf{B}, \tag{2}$$

$$\frac{\partial \mathbf{B}}{\partial t} = \mathrm{curl}(\mathbf{V} \times \mathbf{B}), \tag{3}$$

$$\frac{\partial \rho}{\partial t} + \mathrm{div}(\rho \mathbf{V}) = 0, \tag{4}$$

where the vectors $\mathbf{V}$ and $\mathbf{B}$ are the plasma velocity and the magnetic field, respectively, and ρ is the plasma density. In equation (2), we ignore finite-β effects, as they are not significant for sausage modes of coronal loops (Inglis et al. 2009).

It is natural to use the cylindrical coordinate system, with the z-axis coinciding with the axis of the cylinder, and ϕ and r being the azimuthal and radial coordinates, respectively. Considering linear magnetoacoustic perturbations of the cylindrical equilibrium given by Eq. (1), and taking that in the sausage mode perturbations are independent of the polar angle ϕ, we obtain for the perturbed quantities:

$$\frac{\partial v_r}{\partial t} = \frac{B_0}{\mu_0 \rho_0}\left(\frac{\partial B_r}{\partial z} - \frac{\partial B_z}{\partial r}\right), \tag{5}$$

$$\frac{\partial B_r}{\partial t} = B_0 \frac{\partial v_r}{\partial z}, \tag{6}$$

$$\frac{\partial B_z}{\partial t} = -B_0\left(\frac{\partial v_r}{\partial r} + \frac{v_r}{r}\right), \tag{7}$$

where v_r is the radial component of the plasma velocity, and B_r and B_z are the perturbations of the radial and longitudinal components of the magnetic field, respectively.

Using the standard procedure of the exclusion of all but one perturbed variables from equations (5-7) (see, e.g., the linear part of Nakariakov et al. 1997), we obtain the fast

magnetoacoustic wave equation,

$$\frac{\partial^2 v_r}{\partial t^2} = \frac{B_0^2}{\mu_0 \rho_0(r)} \left(\frac{\partial^2 v_r}{\partial z^2} + \frac{\partial^2 v_r}{\partial r^2} + \frac{1}{r}\frac{\partial v_r}{\partial r} - \frac{v_r}{r^2} \right) \tag{8}$$

for sausage perturbations of the field-aligned plasma cylinder. Slow magnetoacoustic perturbations are absent from this equation, as we ignore the finite-β effects.

As the equilibrium is uniform along the axis of the cylinder, in the z-direction, we can perform the Fourier transform with respect to this coordinate, assuming that the perturbed physical quantities depend upon z as $\cos(k_z z)$. These assumptions, in particular, corresponds to the consideration of standing modes with the longitudinal wavelength $2\pi/k_z$. Thus, we obtain the fast wave equation for the harmonic fast magnetoacoustic perturbations in the longitudinal direction,

$$\frac{1}{C_A^2(r)}\frac{\partial^2 v_r}{\partial t^2} + \left(k_z^2 + \frac{1}{r^2} \right) v_r - \frac{\partial^2 v_r}{\partial r^2} - \frac{1}{r}\frac{\partial v_r}{\partial r} = 0. \tag{9}$$

Eq. (9) contains the explicit dependence upon only two coordinates, the time t and the radial coordinate r. In particular, Equation (9) describes standing sausage waves of wavelength $2\pi/k_z$, which are observed in flaring coronal loops.

An initial value problem is solved with the initial condition

$$V_r(r, t = 0) = A_0 r \exp\left(-r^2/d^2\right) \tag{10}$$

where A_0 is the amplitude. This form of the initial perturbation has the sausage symmetry, as it is independent of the azimuthal angle ϕ and the plasma velocity at the axis of the cylinder is zero. The width of the perturbation in the radial direction is taken sufficiently large to avoid the excitation of higher radial harmonics: the shape of the perturbation is close to the transverse structure of the lowest mode (see, e.g. Pascoe et al. 2007b; Inglis et al. 2009), with one maximum of the radial velocity perturbation in the radial direction. Higher radial sausage harmonics have more than one extremum in the radial direction, and hence are excited by driver (10) less effectively. In the longitudinal direction the initial perturbation is described by a harmonic function with the wavenumber k_z. Eq. (10) is supplemented by the boundary conditions $V_r(r = 0, t) = V_r(r = 50d, t) = 0$.

Evolution of the initial perturbation was numerically calculated using the function *pdsolve* of *Maple* 16, which implements a second order (in space and time) centred finite difference scheme (see Maple User Manual 2012, for details). The convergence of the method was checked by doubling the number of grid points. Performance of this solver, in particular the radial structure of the sausage mode and its period for a given wavelength, was tested by

the comparison with the exact analytical results for a similar problem for a zero-β plasma slab with the symmetric Epstein profile of the density, embedded in a straight magnetic field Cooper et al. (2003). In the cylindrical case, considered in this paper, calculations were carried out in the domain ($0 < r < 50d$, $0 < t < NdC_{A\infty}$), where N is sufficiently large (e.g. $N = 50$) for confident resolution of several periods of oscillations.

Two typical scenarios of the evolution of the initial perturbation, the leaky and trapped, are shown in Fig. 2. The figure shows the time evolution of the radial structure of the initial impulsive perturbation of the harmonic dependence on the longitudinal coordinate, $\cos(k_z z)$ for an arbitrary value of z. It is evident that in the trapped regime the initial excitation remains localised near the axis of the cylinder ($r = 0$) and is evanescent for higher values of r. In contrast, the leaky waves are radiated from the cylinder to the external medium as propagating fast magnetoacoustic waves. However, they can be seen in the cylinder for some time after the excitation as decaying harmonic oscillations.

Analysing the signal at a chosen spatial position, e.g. $r = d$ we get information about its time evolution and hence the period of oscillations and the decay time. As in the leaky regime the signal is quickly decaying, the preferable analytical tool is the fitting of the time signal by an exponentially decaying harmonic function by the least-square method. In this study we restrict our attention to the analysis of the dependence of the period on the parameters of the cylinder and the initial excitation only.

3. Parametric study

3.1. Dependence of the sausage mode period on the longitudinal wavelength

Fig. 3 shows the dependence of the period of sausage oscillations on the wavelength $2\pi/k_z$. In the short wavelength limit the period is determined by the ratio of the longitudinal wavelength to the Alfvén speed at its centre (e.g. Edwin & Roberts 1983). In the figure, it corresponds to the straight line $P = 2\pi/[k_z C_A(r = 0)] = 2\pi/[k_z C_{A\infty}(1 - \delta)]$. With the increase in the wavelength, the period increases, and the effective phase speed is in the range between the Alfvén speed in the centre of the cylinder and at infinity, which is consistent with the reasoning in (Nakariakov et al. 2003). As the wavelength increases, the growth of the period becomes less steep, gradually approaching another asymptote, $P = 2\pi/(k_z C_{A\infty})$, determined by the Alfvén speed outside the cylinder. An important feature of this dependence is the presence of the cut-off value. At the cut-off, the period is equal to the ratio of the wavelength to the value of the Alfvén speed at infinity.

For wavelengths shorter than the cutoff value, the oscillations are trapped, and the

period grows with the increase in the wavelength. This is consistent with the results obtained in the slab geometry (Pascoe et al. 2007b; Inglis et al. 2009). In the weakly-leaky regime, for the wavelengths slightly exceeding the cutoff value, the period still grows with the wavelength (see the right panel of Fig. 3), again in agreement with the slab case. For long wavelengths, the dependence of the period on the wavelength shows saturation, and the period becomes independent of the wavelength. This effect is more pronounced for cylinders with higher ratios of the external to internal Alfvén speeds, in other words, with a deeper potential well in the radial profile of the Alfvén speed. This effect was not found in the slab case (Pascoe et al. 2007b; Inglis et al. 2009), because of the insufficiently long wavelengths in the simulations to see the saturation of the sausage mode period with the wavelength. In all cases considered, for the same values of the wavelength and the Alfvén speed at infinity, the sausage mode periods are always longer for the cylinders with lower internal Alfvén speed. In the considered low-β model, cylinders with lower internal Alfvén speed are the cylinders with denser plasma.

The figure also contains a curve indicating where the damping time is equal to three periods of oscillations. Above this curve, the oscillations are of sufficiently high quality to be easily detectable in the data. Thus, leaky sausage oscillations in long dense loops, with a high ratio of the Alfvén speeds, can be of sufficiently high quality, with the damping time much longer than the period of oscillations. We need to point out that the damping considered here is connected with the wave leakage only. In addition, the sausage mode can be subject to damping connected with various dissipative processes, which also reduce the quality of the oscillations. For example, in hot and dense flaring loops it can be the field-aligned thermal conduction (Zaitsev & Stepanov 1982). This effect is not considered in our study, as our governing equations are ideal.

3.2. Dependence of the sausage mode period on the steepness of the transverse profile

The left panel of Fig. 4 shows the effect of the transverse profile steepness on the sausage mode period. As it is discussed in section 3.1, for the step-function profile, in the short wavelength limit the period is determined by the ratio of the longitudinal wavelength to the Alfvén speed at its centre. Our calculations confirm this result. The same estimation is correct for smooth profiles too. With the increase in the wavelength, the period growth is lower than the short-wavelength asymptote, $P = 2\pi/[k_z C_{A\infty}(1-\delta)]$. For the same wavelength, the periods of sausage oscillations in cylinders with smoother profiles of the Alfvén speed, of lower indices α, are evidently shorter. This effect can be explained as follows: in the case of

the step-function profile, the maximum of the perturbation inside the cylinder is situated at the radial distance where the Alfvén speed is equal to the value at the axis of the cylinder. In cylinders with smoothly-growing radial profiles of the Alfvén speed, its value at that radial distance is higher than at the axis of the cylinder. Hence, the effective phase speed of the sausage oscillations in cylinders with smoothly-growing profiles of the Alfvén speed is higher. For the same longitudinal and radial wavelengths, higher values of the effective phase speed give shorter periods.

Also, for steeper profiles, the cutoff value of the wavelength is found to be bigger. For comparison, we show the analytical result obtained for a cylinder with the step-function profile that corresponds to the limit $\alpha \to \infty$ in our consideration. Hence, as one would intuitively expect, cylinders with steeper profiles are better waveguides for fast magnetoacoustic waves of sausage symmetry.

From the left panel of Fig. 4 we obtain that the effect of the radial steepness of the plasma cylinder on sausage oscillations is rather strong. The difference of the value of the sausage mode period between the cylinders with the Gaussian ($\alpha = 2$) and the step-function ($\alpha \to \infty$) radial profiles exceeds two times for the given parameter δ.

3.3. The long-wavelength limit

In the right panel of Fig. 4 we demonstrate the dependence of the period in the long-wavelength limit, when it becomes independent of the wavelength, on the Alfvén speed (or density) contrast in the cylinder and on the steepness of its radial profile. The period is systematically longer for higher differences between the Alfvén speeds inside and outside the cylinder, and for steeper profiles.

For comparison, we show the analytical result obtained for a cylinder with the step-function profile that corresponds to the limit $\alpha \to \infty$ in our consideration. It gives that in the zero-β limit the period of a long-wavelength sausage mode of a step-function cylinder depends linearly on the value of $1/C_{A0}$,

$$P \approx 2\pi d/2.4 C_{A0}, \tag{11}$$

(e.g Kopylova et al. 2007), which is consistent with our calculations.

It is also evident that for smoother profiles the sausage mode period becomes shorter (see also discussion in Section 3.2). The period grows with the increase in the ratio $C_{A\infty}/C_{A0}$, while for smaller values of the steepness parameter α this dependence departs from the linear one that appears in the $\alpha \to \infty$ cases. For a fixed value of the ratio of the Alfvén speeds,

the period is seen to depend very nonlinearly on the steepness parameter α. In particular, for $C_{A\infty}/C_{A0} = 10$, which is a typical value for flaring loops (e.g. Nakariakov et al. 2003), we get an estimate formula

$$P \approx 26.1 d \tanh(\lg \alpha). \tag{12}$$

It is applicable for the low-β profiles steeper than Gaussian, $\alpha > 2$ and is consistent with the analytical result in the $\alpha \to \infty$ limit.

4. Conclusions

We performed numerical simulations of the azimuthally-symmetric initial value problem for a field-aligned low-β plasma cylinder with a smooth radial profile of the density, (and hence of the Alfvén speed). The plasma cylinder was excited by a symmetric perturbation of the radial velocity of the plasma and of a harmonic shape in the longitudinal direction. Fast magnetoacoustic sausage modes were found to be easily excited in both trapped and leaky regimes. The results obtained can be summarised as follows:

- With the increase in the longitudinal wavelength, the period of the sausage oscillations always grows, while this dependence experiences saturation in the long-wavelength limit.

- In the trapped regime, the period lies between two values, corresponding to the ratio of the effective radius of the cylinder and the Alfvén speed at its axis and at infinity, and grows with the increase in the wavelength.

- For wavelengths greater than the cutoff value, sausage modes become leaky. In response to an impulsive excitation, in the cylinder, the leaky waves show decaying oscillatory behaviour, with the period determined by the parameters of the cylinder (the Alfvén speed contrast ratio and steepness). Outside the cylinder, the leaky waves form a wave-train pattern that propagates outwards at the external Alfvén speed. As expected, deeper and steeper profiles of the Alfvén speed correspond to more efficient trapping of sausage modes: the cutoff value of the wavelength increases with the steepness and the density (or Alfvén speed) contrast ratio.

- In the leaky regime, the period is always longer than the period of a trapped mode of a shorter wavelength, and also is longer than the cutoff value: the ratio of the wavelength and the Alfvén speed far from the cylinder. For shallow profiles of the density (and hence the Alfvén speed) and shorter wavelengths, the period grows with the wavelength in the leaky regime too. In the long wavelength limit, the period becomes independent

of the wavelength and is determined by the depth and steepness of the radial profile of the Alfvén speed: the period is approximately inversely proportional to the internal value of the Alfvén speed, and depends on the steepness index α as $\tanh(\lg \alpha)$.

Our findings resolve the long-standing problem of the dependence or independence of the period of the sausage oscillations on the wavelength. Indeed, for shorter wavelengths, even in the leaky regime, the period grows with the wavelength. In particular, for thick flaring coronal loops with the density contrast of about 10 (and hence with the Alfvén speed contrast ratio of about 3.16) and the length of about 5-6 its diameters, considered by Nakariakov et al. (2003); Aschwanden et al. (2004) the period of the fundamental sausage mode indeed increases with the wavelength. But for longer wavelengths (and higher density contrast ratios), the dependence of the period on the wavelength experiences the saturation, and becomes consistent with the analytical results obtained by Zaitsev & Stepanov (1982); Kopylova et al. (2002, 2007). Thus, we infer that the previously-made opposite conclusions on the dependence of the sausage mode period on the wavelength were drawn in different ranges of the problem parameters, and hence do not contradict each other. More specifically, the regime described in (Pascoe et al. 2007b; Inglis et al. 2009) corresponds to the segments of the solid and dashed curves near the thick solid line in Fig. 3, right panel. On the other hand, the regime described in (Zaitsev & Stepanov 1982; Kopylova et al. 2002, 2007) corresponds to the saturation of the curves in the long-wavelength part of that figure.

This result has important implications for the seismological diagnostics of plasmas in flaring loops with the use of sausage oscillations. In particular, the pronounced dependence of the sausage oscillation period on the steepness of the radial profile of the Alfvén speed provides us with a tool for probing that parameter. The transverse steepness is vital for the assessment of the efficiency of kink wave damping in the solar corona (see, e.g. Goossens et al. 2012, and references therein) and of associated coronal heating. An additional advantage of seismological techniques utilising the sausage mode is provided by its independence of the length of the loop in the long-wavelength regime. It allows one to exclude this parameter from consideration in the diagnostics of long dense loops. Moreover, equation (12) gives us with a tool for probing the transverse profile of the Alfvén speed and the density in the sausage-oscillating coronal loop, provided we are able to get an independent measurements of loop diameter d and the Alfvén speed C_{A0}. In particular, the latter parameter can come from the observation of a kink oscillation of the same loop.

The work was supported by the Royal Society UK-Russian International Joint Project, the Marie Curie PIRSES-GA-2011-295272 RadioSun project, and the Russian FCPK-1.5 No.8524 project. VFM acknowledges the grants of the Russian Foundation for Basic Research

02-11-91175 and 02-12-00616.

REFERENCES

Aschwanden, M. J., Nakariakov, V. M., & Melnikov, V. F. 2004, ApJ, 600, 458

Banerjee, D., Erdélyi, R., Oliver, R., & O'Shea, E. 2007, Sol. Phys., 246, 3

Cally, P. S. 1986, Sol. Phys., 103, 277

Cooper, F. C., Nakariakov, V. M., & Williams, D. R. 2003, A&A, 409, 325

De Moortel, I., & Nakariakov, V. M. 2012, Royal Society of London Philosophical Transactions Series A, 370, 3193

Edwin, P. M., & Roberts, B. 1983, Sol. Phys., 88, 179

Goossens, M., Andries, J., Soler, R., et al. 2012, ApJ, 753, 111

Gruszecki, M., Nakariakov, V. M., & Van Doorsselaere, T. 2012, A&A, 543, A12

Inglis, A. R., Nakariakov, V. M., & Melnikov, V. F. 2008, A&A, 487, 1147

Inglis, A. R., van Doorsselaere, T., Brady, C. S., & Nakariakov, V. M. 2009, A&A, 503, 569

Kopylova, Y. G., Melnikov, A. V., Stepanov, A. V., Tsap, Y. T., & Goldvarg, T. B. 2007, Astronomy Letters, 33, 706

Kopylova, Y. G., Stepanov, A. V., & Tsap, Y. T. 2002, Astronomy Letters, 28, 783

Maple User Manual, Waterloo Maple Inc. 2012, http://www.maplesoft.com/documentation_center

Mathioudakis, M., Seiradakis, J. H., Williams, D. R., et al. 2003, A&A, 403, 1101

Melnikov, V. F., Reznikova, V. E., Shibasaki, K., & Nakariakov, V. M. 2005, A&A, 439, 727

Mossessian, G., & Fleishman, G. D. 2012, ApJ, 748, 140

Nakariakov, V. M., & Melnikov, V. F. 2009, Space Science Reviews, 55

Nakariakov, V. M., Melnikov, V. F., & Reznikova, V. E. 2003, A&A, 412, L7

Nakariakov, V. M., Roberts, B., & Murawski, K. 1997, Sol. Phys., 175, 93

Pascoe, D. J., Nakariakov, V. M., & Arber, T. D. 2007, Sol. Phys., 246, 165

Pascoe, D. J., Nakariakov, V. M., & Arber, T. D. 2007, A&A, 461, 1149

Pascoe, D. J., Nakariakov, V. M., Arber, T. D., & Murawski, K. 2009, A&A, 494, 1119

Roberts, B., Edwin, P. M., & Benz, A. O. 1984, ApJ, 279, 857

Rosenberg, H. 1970, A&A, 9, 159

Ruderman, M. S., & Roberts, B. 2006, Sol. Phys., 237, 119

Selwa, M., Murawski, K., & Kowal, G. 2004, A&A, 422, 1067

Srivastava, A. K., Zaqarashvili, T. V., Uddin, W., Dwivedi, B. N., & Kumar, P. 2008, MNRAS, 388, 1899

Stepanov, A. V., Zaitsev, V. V., & Nakariakov, V. M. 2012, Coronal Seismology (1st ed.; Weinheim: Wiley-VCH Verlag)

Su, J. T., Shen, Y. D., Liu, Y., Liu, Y., & Mao, X. J. 2012, ApJ, 755, 113

Van Doorsselaere, T., De Groof, A., Zender, J., Berghmans, D., & Goossens, M. 2011, ApJ, 740, 90

Verwichte, E., Foullon, C., & Nakariakov, V. M. 2006, A&A, 449, 769

Zaitsev, V. V. & Stepanov, A. V. 1975, Issled. Geomagn. Aeron. Fiz. Solntsa, 37, 3

Zaitsev, V. V., & Stepanov, A. V. 1982, Soviet Astronomy Letters, 8, 132

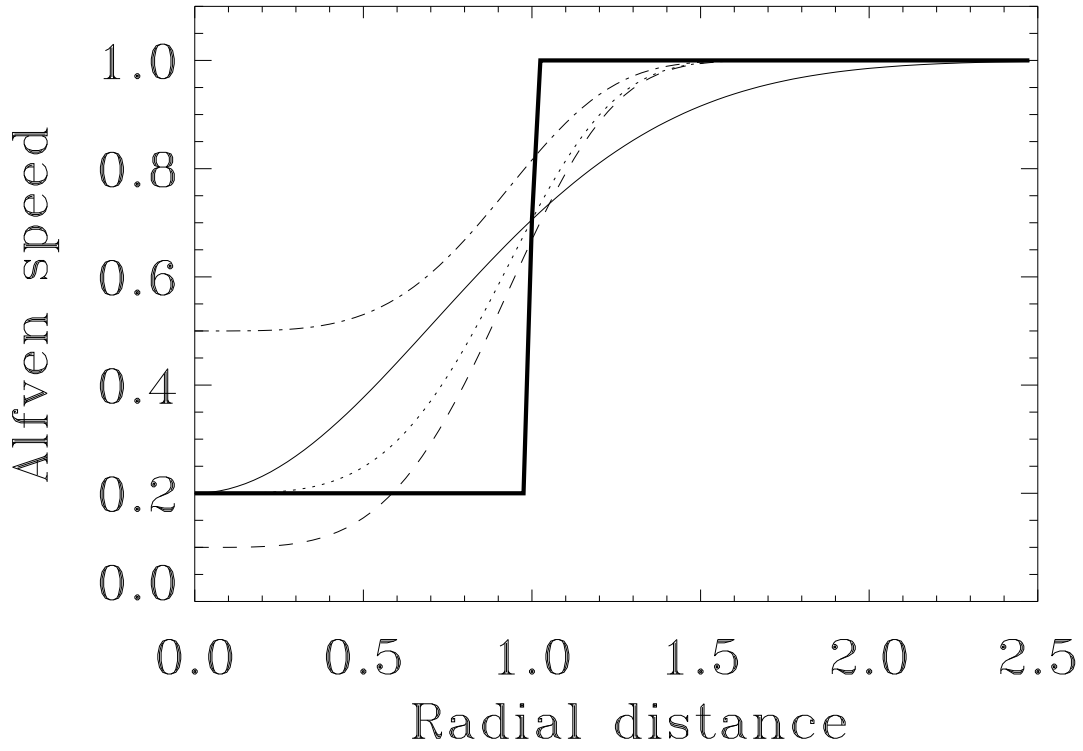

Fig. 1.— Examples of the radial profiles of the Alfvén speed in the considered plasma cylinder, for different values of the parameters α and δ, which control the steepness and depth of the profile, respectively. The thick solid curve corresponds to $\alpha = \infty$, $\delta = 0.8$; the thin solid curve to $\alpha = 2$, $\delta = 0.8$; the dotted curve to $\alpha = 4$, $\delta = 0.8$; the dashed curve to $\alpha = 4$, $\delta = 0.9$; and the dot-dashed curve to $\alpha = 4$, $\delta = 0.5$. The Alfvén speed is normalised to its value at infinity, and the radial distance to the effective radius of the cylinder.

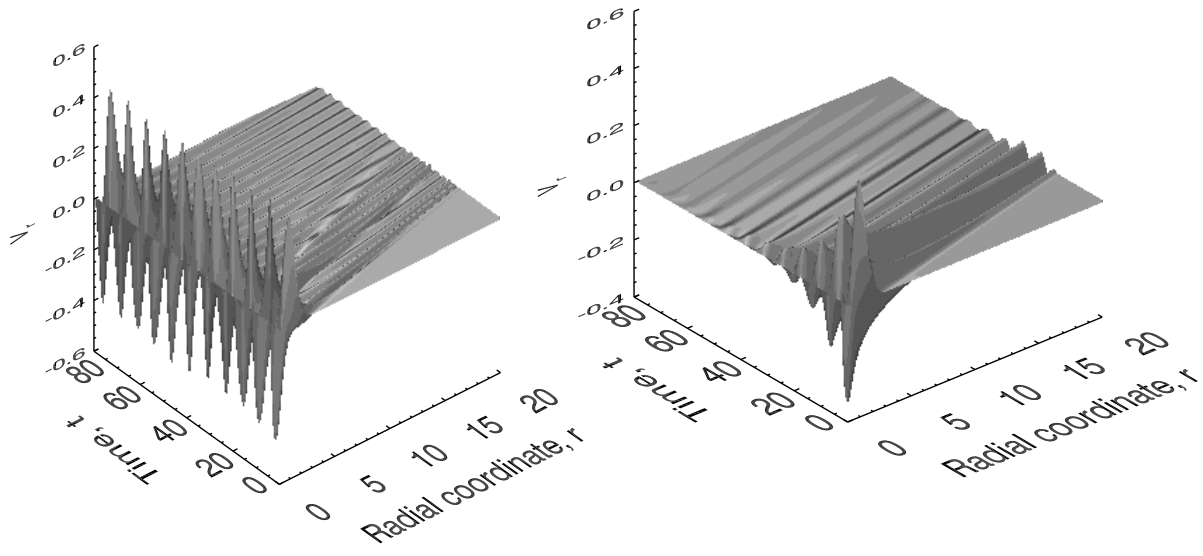

Fig. 2.— *Left panel:* Example of a trapped oscillation, obtained for the parameters: $k_z = 1.5$, $\delta = 0.8$, $\alpha = 6$. *Right panel:* Example of a leaky oscillation, for: $k_z = 0.4$, $\delta = 0.7$, $\alpha = 6$. The time is measured in $d/C_{A\infty}$, and the radial distance in d. The vertical axis shows the radial component of the plasma velocity measured in units of the initial amplitude A_0.

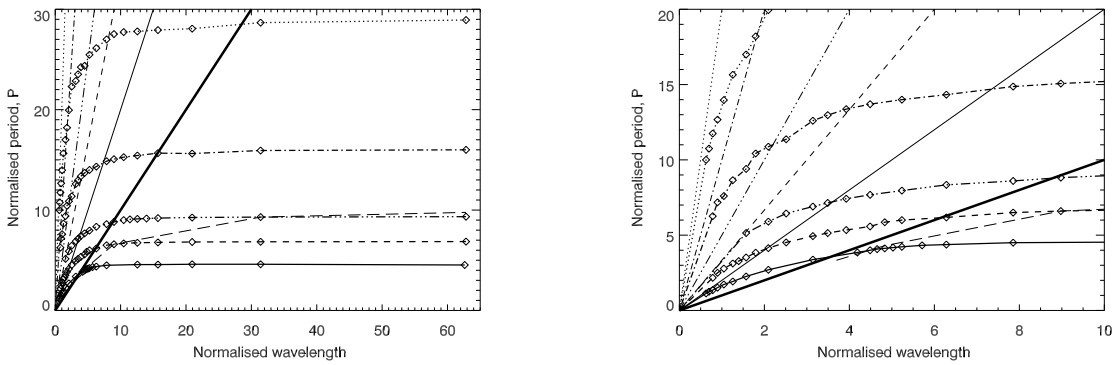

Fig. 3.— *Left panel:* Dependence of the period of oscillations on the wavelength $2\pi/k_z$, for different values of the parameter δ that is connected with the density contrast inside and outside the cylinder. Dotted curve shows the case of $\delta = 0.95$, dot-dashed curve $\delta = 0.9$, triple dot-dashed $\delta = 0.8$, dashed $\delta = 0.7$ and the solid line is for $\delta = 0.5$. The diamonds represent the specific measurements. The value of α is 6 for all curves. The thick straight line shows the cutoff, $P = 2\pi/(k_z C_{A\infty})$. Other straight lines show the values of $P = 2\pi/[k_z C_{A\infty}(1-\delta)]$ for the various values of δ. The long dashed line shows where the damping time is equal to three periods of oscillations. The period is measured in units of $d/C_{A\infty}$, and the wavelength in units of d. *Right panel:* The same as in the left panel, but zoomed to show the trapped regime.

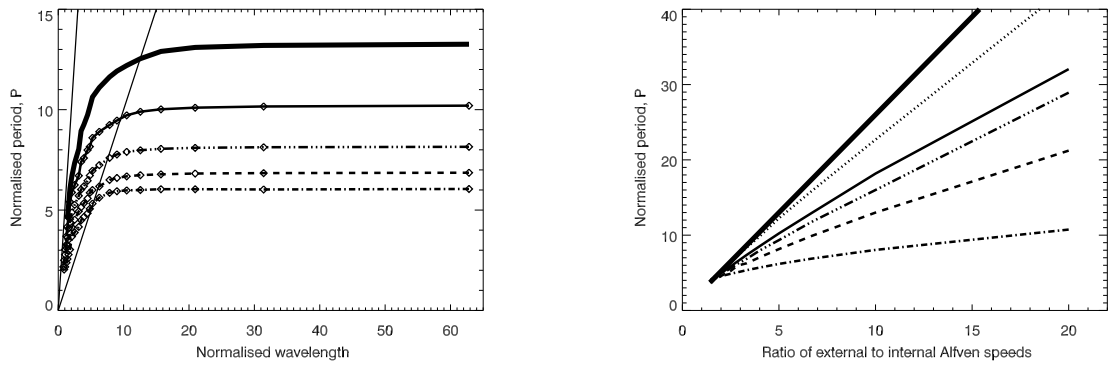

Fig. 4.— *Left panel:* Dependence of the period of oscillations on the wavelength for different steepnesses of the radial profile α. The thick solid line corresponds to $\alpha = \infty$, the think solid line to $\alpha = 8$, the triple dot-dashed line to $\alpha = 6$, the dashed line to $\alpha = 4$, and the dot-dashed line to $\alpha = 2$. The value of δ is 0.8 for all curves. The straight lines are the cutoffs $P = 2\pi/(k_z C_{A\infty})$ and $P = 2\pi/[k_z C_{A\infty}(1-\delta)]$. *Right panel:* Dependence of the period in the long wavelength limit, on the ratio of external to internal Alfvén speeds, for different steepnesses. The dotted curve corresponds to $\alpha = 20$. The other curve styles are the same as in the left panel. The thick solid line shows the analytical solution in the long-wavelength limit for the step-function profile. In both panels, the period is measured in units of $d/C_{A\infty}$, and the wavelength in units of d.